

Structural investigation of the quasi-one-dimensional reconstructions induced by Eu adsorption on a Si(111) surface

Kazuyuki Sakamoto,^{1,*} A. Pick,² and R. I. G. Uhrberg²

¹*Department of Physics, Graduate School of Science, Tohoku University, Sendai 980-8578, Japan*

²*Department of Physics and Measurement Technology, Linköping University, S-581 83 Linköping, Sweden*

(Received 26 July 2005; published 29 November 2005)

The surface structures of the (quasi-)one-dimensional reconstructions induced by the adsorption of Eu on Si(111) have been investigated by low-energy electron diffraction (LEED) and high-resolution core-level photoelectron spectroscopy. Different phases were observed in LEED depending on the Eu coverage. The lowest coverage phase has a (3×2) periodicity, and the highest coverage phase has a (2×1) one. Of the intermediate phases, the LEED pattern of the so-called (5×1) surface indicates that this surface has actually a (5×4) periodicity. The Eu $4f$ core-level spectra show that the Eu coverages of the (3×2) , (5×4) , and (2×1) phases are $1/6$ monolayer (ML), 0.3 ML, and 0.5 ML, respectively, and that the valence state of the adsorbate is $2+$ in all these three phases. In the Si $2p$ core-level spectra, three surface components were observed in both the lowest and highest coverage phases. By considering the energy shift and intensity of each surface component, we conclude that the structure of the (3×2) phase is basically the same as that of the honeycomb-chain-channel model, and that the (2×1) phase is formed by π -bonded Seiwatz Si chains. Regarding the (5×4) phase, two extra Si $2p$ surface components were observed together with the three components observed in the two end phases. Taking the energy shifts and intensities of the extra surface components into account, we propose a structural model of the (5×4) phase.

DOI: [10.1103/PhysRevB.72.195342](https://doi.org/10.1103/PhysRevB.72.195342)

PACS number(s): 68.35.-p, 79.60.-i, 61.14.Hg, 68.43.-h

I. INTRODUCTION

Motivated by the technological importance to make nanometer-scale electronic devices, self-assembling one-dimensional (1D) superstructures, which are formed on semiconductor surfaces by the adsorption of metal atoms, is a topic of increasing interest. From a scientific point of view, these 1D structures have attracted much attention due to the possibility of observing various exotic physical phenomena, such as formations of non-Fermi-liquid-like ground states, Peierls-like phase transitions, or order-disorder transitions.¹⁻⁶ The 1D and quasi-1D reconstructions formed by the adsorption of rare-earth metals (REMs) on a Si(111) surface⁷⁻¹⁶ are candidates for such 1D systems.

The Eu/Si(111) surface has been reported to form a quasi-1D (3×2) reconstruction at a coverage of $1/6$ ML, and a series of 1D $[(n \times 1); n=5, 7, \text{ and } 9]$ reconstructions at higher coverages that culminates with a (2×1) phase at 0.5 ML.¹⁰⁻¹⁴ Of these reconstructions, the lowest coverage (3×2) phase has been proposed to have the same atomic structure as that of alkaline-earth metal (AEM) induced Si(111)- (3×2) surface¹⁷⁻²⁵ in Refs. 11-15. That is, the structure is basically the same as that of the honeycomb-chain-channel (HCC) model,²⁶⁻²⁸ which was originally proposed for $1/3$ ML monovalent atom induced Si(111)- (3×1) reconstructions, but with an adsorbate coverage of $1/6$ ML [Fig. 1(a)]. Concerning the other Eu/Si(111) phases, the highest coverage (2×1) phase was proposed to be formed by π -bonded Seiwatz Si chains²⁹ [Fig. 1(b)] likewise the AEM induced Si(111)- (2×1) surface^{20,23,30-32} in Refs. 13 and 15. The surface electronic structures of the two end phases support indirectly these propositions.¹⁵ However, the (3×2) phase is obtained experimentally with an Eu coverage of 0.2

ML in Refs. 12-14, and the (2×1) phase is obtained experimentally with an Eu coverage of 0.7 ML in Refs. 12 and 13. These results indicate that the proposed models are still questionable, and thus that further investigations are necessary. Moreover, even though the intermediate phases [the (5×1) , (7×1) , and (9×1) phases] were proposed to be formed by combinations of the HCC model and the Seiwatz model as well as the AEM's induced reconstructions,¹²⁻¹⁴ the structural models proposed for the (5×1) phase [Fig. 1(c)] is slightly different from those proposed for the AEM's induced Si(111)- (5×1) surfaces.^{20,25}

In this paper, we present detailed low-energy electron diffraction (LEED) and high-resolution core-level photoelectron spectroscopy measurements of the 1D and quasi-1D reconstructions induced by the adsorption of Eu on a Si(111) surface. LEED gives information about the periodicity of the surface structure, and high-resolution core-level photoelectron spectroscopy gives information about not only the atomic structure of the surface, but also about the charge states of the surface atoms. In the LEED study, we obtained that the periodicities of the lowest and highest coverage phases are (3×2) and (2×1) , respectively, and that the so-called (5×1) surface has actually a (5×4) periodicity. The Eu coverages of the (3×2) , (5×4) , and (2×1) phases are $1/6$ ML, 0.3 ML, and 0.5 ML, respectively, and the valence state of the adsorbate is Eu^{2+} in these three phases. Taking the energy shifts and intensities of the Si $2p$ surface components into account, we conclude that the basic structure of the (3×2) phase follows the HCC model, and the (2×1) phase is formed by Seiwatz Si chains. These results strongly support the structures of the Eu/Si(111)- (3×2) and (2×1) surfaces proposed in the literature. Together with the three components observed in the two end phases, two extra Si $2p$

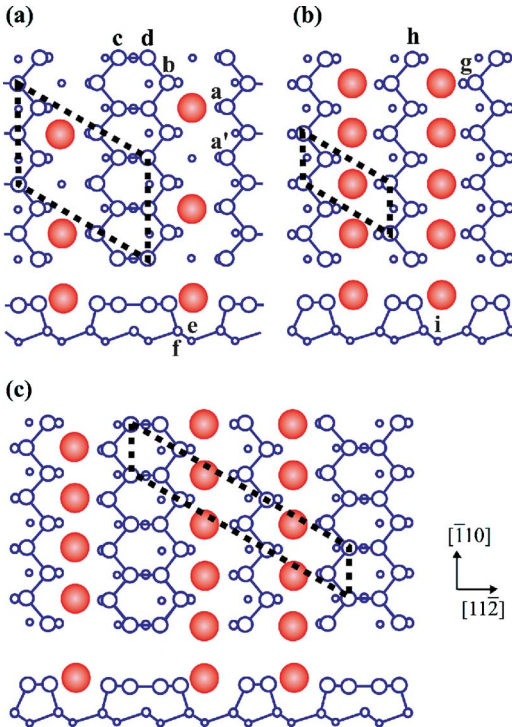


FIG. 1. (Color online) (a) HCC structure of the Si(111)-(3 \times 2) surface with an adsorbate coverage of 1/6 ML. (b) Seiwatz structure of the Si(111)-(2 \times 1) surface with an adsorbate coverage of 0.5 ML. (c) Structural model of the so-called Eu/Si(111)-(5 \times 1) surface proposed in the literature. Filled circles are metal atoms, which are adsorbed on the T_4 site, and open circles are Si atoms. The dashed lines indicate the unit cell of each surface.

surface components were observed in the intermediate (5 \times 4) phase. By considering the energy shifts and the intensities of the extra surface components and by taking the adsorbate coverage into account, a structural model of the (5 \times 4) phase is proposed.

II. EXPERIMENTAL DETAILS

The high-resolution photoemission measurements and LEED studies were performed at Beamline 33 at the MAX-I synchrotron radiation facility in Lund, Sweden. The Eu 4*f* and Si 2*p* core-level spectra were obtained with an angle-resolved photoelectron spectrometer with an angular resolution of $\pm 2^\circ$. The total experimental energy resolutions were ~ 200 meV for the Eu 4*f* measurements and ~ 80 meV for the Si 2*p* measurements. The Si(111) sample, cut from an Sb-doped (*n* type, 3 Ω cm) Si wafer, was preoxidized chemically before it was inserted into the vacuum system. To obtain a clean surface, we annealed the sample at 1230 K by direct resistive heating in the vacuum chamber to remove the oxide layer, and at 1520 K to remove carbon contamination from the surface. After the annealing, a sharp (7 \times 7) LEED pattern was observed, and neither the valence-band spectra nor the Si 2*p* core-level spectra showed any indication of contamination. Each Eu induced reconstruction was prepared by either depositing a certain amount of Eu onto the clean

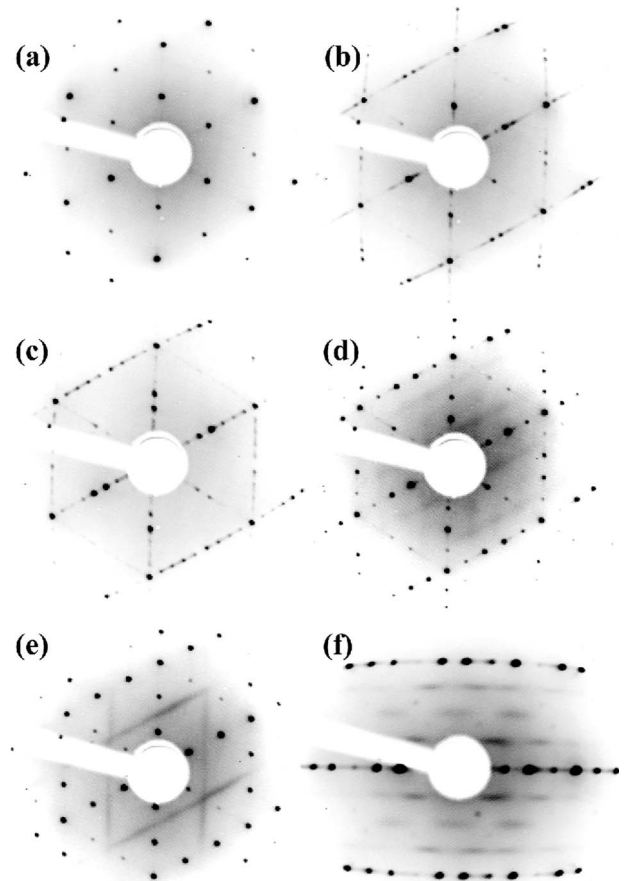


FIG. 2. LEED patterns of the Eu/Si(111) surfaces obtained at different coverages. Eu coverage decreases in the order of (a) \rightarrow (b) \rightarrow (c) \rightarrow (d) \rightarrow (e). Primary electron energies are (a) 82 eV, (b) 82 eV, (c) 69 eV, (d) 82 eV, and (e) 82 eV. The patterns in (a)–(e) are obtained at 300 K. (f) shows the LEED pattern of a single domain so-called Si(111)-(5 \times 1) surface observed at 100 K.

Si(111)-(7 \times 7) surface that was subsequently annealed at approximately 1000 K, or by reducing the Eu coverage by annealing the 0.5 ML Eu adsorbed Si(111)-(2 \times 1) surface at a temperature between 1000 and 1150 K.

III. RESULTS

A. LEED

Figures 2(a)–2(e) show the LEED patterns of the Eu/Si(111) phases formed at different adsorbate coverages. The LEED pattern of the highest coverage phase is displayed in Fig. 2(a), and the Eu coverage decreases in the order of (a) \rightarrow (b) \rightarrow (c) \rightarrow (d) \rightarrow (e). Figures 2(a)–2(c) show the LEED pattern of the Eu/Si(111)-(2 \times 1) and (9 \times 1) surfaces, and Fig. 2(b) displays the pattern of the Eu/Si(111)-(11 \times 1) surface that was not reported in previous studies. In Fig. 2(e), $\times 2$ streaks are clearly observed together with the $\times 3$ spots. This result agrees well with the previous studies,^{10–15} in which the lowest coverage phase was reported to have a (3 \times 2) periodicity. In Fig. 2(d), dim streaks are observed together with sharp $\times 5$ spots. Since no trace of other phases [e.g., spots originating from a (3 \times 2) phase] is ob-

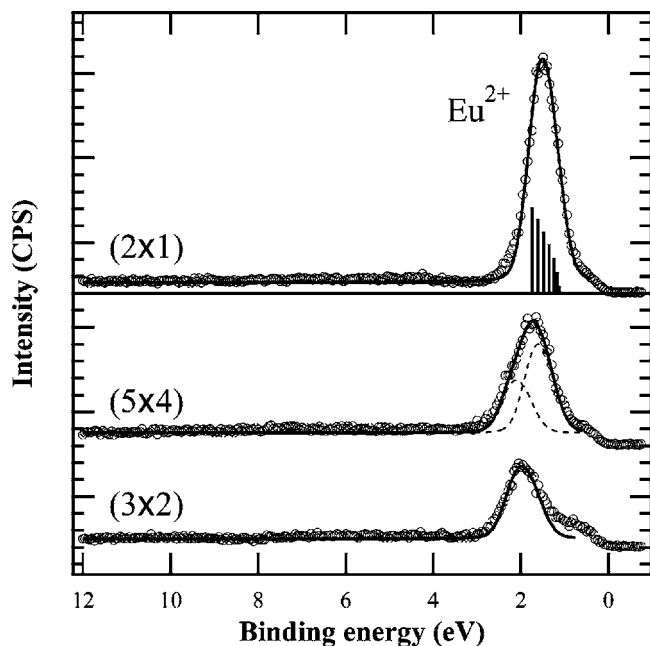


FIG. 3. Eu $4f$ core-level spectra of the Eu/Si(111)- (2×1) , (5×4) , and (3×2) surfaces measured at 300 K with $h\nu=80$ eV. Open circles are the experimental data, and the solid line overlapping the experimental spectrum of the (2×1) phase is the calculated spectrum, which is obtained using the position and relative intensity of multiplet structures for the $\text{Eu}^{2+} 4f$ final states (Ref. 33) that are indicated with vertical lines. The solid line overlapping the spectrum of the (3×2) phase is the calculated $\text{Eu}^{2+} 4f$ peak, and the solid line overlapping the spectrum of the (5×4) phases is the fitting result obtained using the two calculated $\text{Eu}^{2+} 4f$ peaks indicated by dashed lines.

served in Fig. 2(d), these dim streaks originate from the so-called Eu/Si(111)- (5×1) surface itself. In order to obtain a clearer picture about these dim streaks, we have made a single domain sample and cooled it down. Figure 2(f) shows the LEED pattern of a single domain so-called Eu/Si(111)- (5×1) surface obtained at 100 K. The positions of the streaks observed in Fig. 2(f) indicate that this surface has actually a (5×4) periodicity, and thus that this intermediate phase is not formed by a simple combination of the (3×2) and (2×1) phases. Further, the observation of the (5×4) phase suggests that the other intermediate phases [the (7×1) phase, which is not shown here, the (9×1) phase, and the (11×1) phase] might not just be simple combinations of the two end phases, but may also have $\times 4$ periodicities along the chains. The long distances between the chains lead to very weak correlation between the neighboring $\times 4$ periodic chains, which could explain the absence of any $\times 4$ spots and/or $\times 4$ streaks in the LEED patterns of the (9×4) and (11×4) phases in Fig. 2.

B. Eu $4f$ core level

Since valence fluctuation phenomena occur in Eu compounds, it is important to understand the valence states of the adsorbate of the Eu/Si(111) surfaces. Figure 3 shows the Eu

$4f$ core-level spectra (open circles) of the (2×1) , (5×4) , and (3×2) phases measured at 300 K with a photon energy ($h\nu$) of 80 eV and an emission angle (θ_e) of 0° , i.e., normal emission. The Eu core-level spectra were normalized using the background intensities, which are proportional to the photon flux. A prominent peak is observed at a binding energy (E_B) of 1.5 eV in the spectrum of the (2×1) phase. In order to analyze this peak, we have convoluted the calculated $\text{Eu}^{2+} 4f$ final states,³³ whose multiplet structures are indicated by vertical lines, using Voigt functions. The good agreement between the calculated $\text{Eu}^{2+} 4f$ spectrum (solid line) and the experimental data indicates that this peak mainly originates from the $\text{Eu}^{2+} 4f$ core level. The small structure at the lower binding side of the $\text{Eu}^{2+} 4f$ peak would result from the valence band electronic structure of the Eu/Si(111)- (2×1) surface. The binding energy of the $\text{Eu}^{3+} 4f$ core level is reported to be approximately 6 eV higher than that of the $\text{Eu}^{2+} 4f$ core level in Eu compounds,³⁴ and since no remarkable structure is observed at binding energies higher than the $\text{Eu}^{2+} 4f$ peak, we conclude that the valence state of Eu is 2+ on the (2×1) surface.

The $\text{Eu}^{2+} 4f$ peak is observed at $E_B \sim 1.75$ eV in the spectrum of the (5×4) phase, and at $E_B \sim 2.0$ eV in the spectrum of the (3×2) phase. At the lower binding energy sides of these $\text{Eu}^{2+} 4f$ peaks, small structures that result from the valence band electronic structures are observed likewise the spectrum of the (2×1) phase. Although the $\text{Eu}^{2+} 4f$ peak slightly shifts to higher binding energies as the adsorbate coverage decreases, no clear structure is observed at binding energies corresponding the $\text{Eu}^{3+} 4f$ core level. We, therefore, conclude that the valence state of the adsorbate is 2+ on the Eu/Si(111)- (5×4) and (3×2) surfaces as well as that on the (2×1) phase. This result is consistent with the recent photoemission study,¹⁴ in which Eu atoms are reported to be divalent in the (3×2) phase and the intermediate phases.

The full width at half maximum (FWHM) of the $\text{Eu}^{2+} 4f$ peak of the (3×2) phase is almost the same as that of the (2×1) phase, whereas the FWHM of the $\text{Eu}^{2+} 4f$ peak of the (5×4) phase is approximately 1.3 times larger than that of the (2×1) phase. In order to understand the origin of this difference, we have analyzed the spectra of the (5×4) and (3×2) phases using calculated $\text{Eu}^{2+} 4f$ peaks that have the same shape and same FWHM as those of the (2×1) phase, but different binding energies. The solid lines overlapping the spectra of the (3×2) and (5×4) phases are the fitting results. As shown in Fig. 3, the spectrum of the (3×2) phase is well reproduced by one calculated peak while two calculated peaks (dashed lines) are needed for the (5×4) phase. This result suggests that there are at least two Eu adsorption sites on the (5×4) phase.

C. Si $2p$ core level

Figure 4 shows the Si $2p$ core-level spectra of the Eu/Si(111)- (2×1) , (5×4) , and (3×2) surfaces, measured using different $h\nu$ and θ_e that give a difference in the surface sensitivity. Without any processing, the spectra of the (3×2) phase reveal the presence of several components that

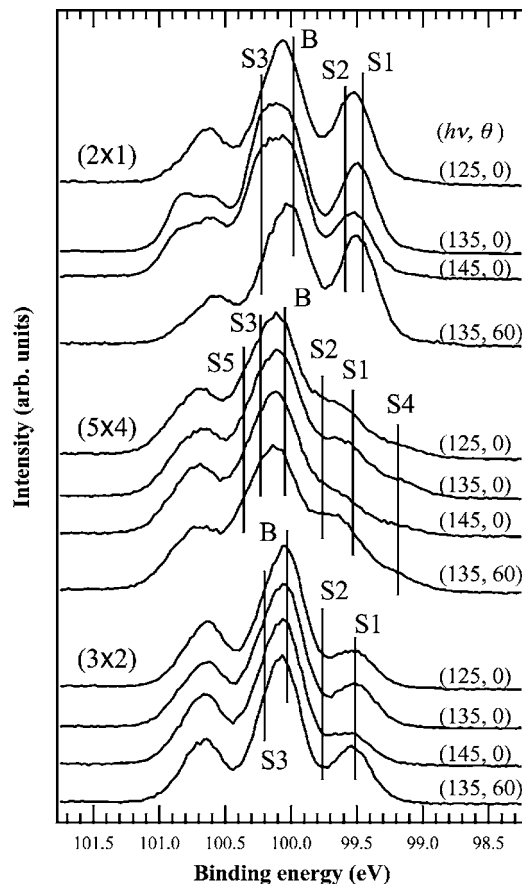


FIG. 4. Si $2p$ core-level spectra of the Eu/Si(111)-(2 \times 1), (5 \times 4), and (3 \times 2) surfaces measured at different $h\nu$ and θ_e . The solid lines indicate the energy positions of the Si $2p_{3/2}$ parts of the four components for the (2 \times 1) and (3 \times 2) phases and of the six components for the (5 \times 4) phase.

contribute to the shape of the spectra. The most evident one is S1, whose $2p_{3/2}$ component is clearly observed at $E_B = 99.55$ eV. The presence of S2 is revealed by the behavior of the valley between the $2p_{3/2}$ components of S1 and B. That is, the flat part observed between $E_B = 99.55$ eV and 99.75 eV in the spectrum obtained using $(h\nu, \theta_e) = (145 \text{ eV}, 0^\circ)$ is impossible to reproduce by using only S1. The contribution from a third component (S3) is confirmed by the asymmetric shape of the largest peak in the spectra obtained using $(h\nu, \theta_e) = (135 \text{ eV}, 0^\circ)$. The presence of three surface components is also revealed for the (2 \times 1) phase. The $2p_{3/2}$ component of S3 is observed as a shoulder at around $E_B = 100.25$ eV and its $2p_{1/2}$ component is clearly observed as a peak at around $E_B = 100.85$ eV. The presences of S1 and S2 are confirmed by the $(h\nu, \theta_e)$ -dependent shift in binding energy of the peak at around $E_B = 99.5$ eV.

Taking its complicated spectral shape into account, one easily concludes that the number of surface components of the (5 \times 4) phase is larger than those of the (3 \times 2) and (2 \times 1) phases. S1 is observed as a small peak at around $E_B = 99.55$ eV using $(h\nu, \theta_e) = (135 \text{ eV}, 0^\circ)$. S2 is revealed by the behavior of the intensity between the $2p_{3/2}$ components of S1 and B. The presence of S3 is obvious from the asymmetric shape of the largest peak. S4 is obvious from the

observation of the peak at around 99.2 eV in the spectra obtained using $h\nu = 135$ eV, and the small structure at the same E_B in other spectra. The contribution from a fifth component S5 is deduced by the long tail on the high binding energy side that extends to 101.3 eV in the spectrum obtained using $(h\nu, \theta_e) = (135 \text{ eV}, 60^\circ)$.

IV. DISCUSSION

Quantitative information about the structures of the Eu/Si(111) surfaces is obtained by analyzing the Si $2p$ spectra by a standard least-squares-fitting method using spin-orbit split Voigt functions. Figure 5 shows the results of the analysis for the Si $2p$ core-level spectra of the Eu/Si(111)-(2 \times 1), (5 \times 4), and (3 \times 2) surfaces obtained using $(h\nu, \theta_e) = (135 \text{ eV}, 60^\circ)$ and $(145 \text{ eV}, 0^\circ)$. The open circles are the experimental data and the solid lines overlapping the data are the fitting curves. We used 608 meV for the spin-orbit splitting and a 80 meV FWHM for the Lorentzian contribution for all components in the fitting procedure. The Gaussian widths of the bulk components are 230 meV (FWHM) in the spectra obtained using $h\nu = 135$ eV and 245 meV (FWHM) in those obtained using $h\nu = 145$ eV. The Gaussian widths of the surface components are between 245 and 280 meV. A polynomial background was subtracted before the decomposition of each spectrum, and each component is indicated by different hatching. The residual between the experimental data and fitting result is indicated at the bottom of each spectrum.

From the result of the fitting procedure, we can conclude that both the (3 \times 2) and (2 \times 1) phases have three surface components, the same number as that reported for the Ca induced Si(111)-(3 \times 2) and (2 \times 1) surfaces.²⁰ This number is also the same as the number of major surface components reported for the Ba/Si(111)-(3 \times 2) and (2 \times 8) surfaces.²⁵ Concerning the (5 \times 4) phase, we can conclude that the number of surface components of this phase is five, i.e., the same number as that of the Ca/Si(111)-(5 \times 2) surface.²⁰ Among the surface components, S1 is observed at the same relative binding energy in the three phases. The binding energy of the S1 component is ~ -510 meV relative to the binding energy of the B component. S2 is observed in all phases with a shift to lower relative binding energies as the coverage of Eu increases. The relative binding energy of S2 is ~ -195 meV in the (3 \times 2) phase, ~ -295 meV in the (5 \times 4) phase, and ~ -370 meV in the (2 \times 1) phase. S3, whose relative binding energy is ~ 185 meV in the (3 \times 2) and (5 \times 4) phases, shifts to a relative binding energy of ~ 250 meV in the (2 \times 1) phase. The close relative binding energies of S1–S3 indicate that the origin of each component is the same or quite similar in the three phases. The relative binding energies of the S4 and S5 components, which are observed in the intermediate (5 \times 4) phase only, are ~ -835 meV and ~ 320 meV. The number of surface components observed in the (3 \times 2) and (5 \times 4) phases and their relative binding energies agree with those reported recently for the two corresponding phases.¹⁴

A. Eu/Si(111)-(3 \times 2)

To investigate the atomic structure of the (3 \times 2) phase, we compare the present result with the former Si $2p$ core-

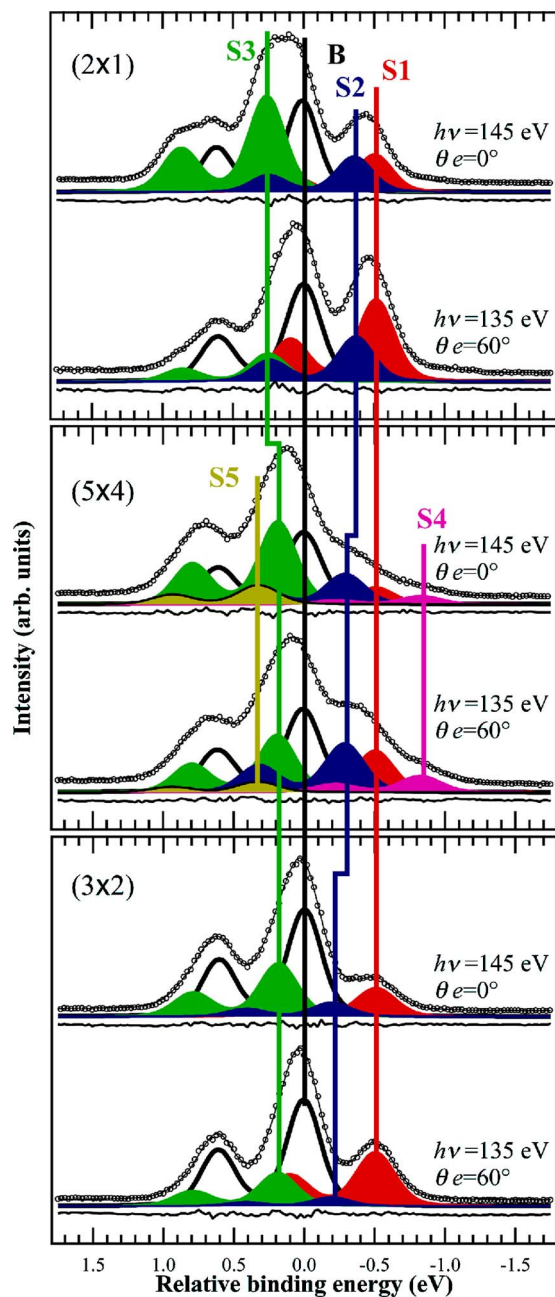


FIG. 5. (Color online) Decomposition of the Si 2*p* core-level spectra of the Eu/Si(111)-(2×1), (5×4), and (3×2) surfaces. The open circles are the experimental data, and the solid lines overlapping the open circles are the fitting curves. Each component is indicated by different hatching. The residual between the experimental data and fitting result is shown by a solid line at the bottom of each spectrum.

level studies performed on the 1/6 ML Ca²⁰ and Ba²⁵ induced Si(111)-(3×2) surfaces. Three surface components, whose relative binding energies are similar to those observed on the (3×2) phase in Fig. 5, are observed on both the Ca/Si(111)-(3×2) and the Ba/Si(111)-(3×2) surfaces. The observation of the same number of surface components and their similar relative binding energies support the proposition^{11–15} that the basic structure of the Eu/Si(111)-(3×2) surface is HCC. Further, the adsorbate coverage of

1/6 ML and the 2+ valence state of Eu strongly support the proposition¹⁸ that the HCC structure is stabilized by the donation of two electrons per (3×2) unit cell.

Based on the Si 2*p* core levels of the alkali metal induced Si(111)-(3×1) surfaces,^{28,35} the two surface components, whose binding energies are lower than that of the bulk component, were attributed to originate from surface Si atoms that face the adsorbate in the studies performed on AEM's induced (3×2) surfaces.^{20,25} However, different intensity ratios were reported in the former studies on AEM's induced surfaces for these two Si 2*p* components. An intensity ratio of 2:1 was reported for the Ca/Si(111)-(3×2) surface,²⁰ while an intensity ratio of 1:1 was reported for the Ba/Si(111)-(3×2) surface.²⁵ In Ref. 25, this difference has been proposed to originate from a diffraction effect, i.e., the intensity ratio reported for the Ca induced reconstructed surface has been proposed to be affected by diffraction due to the smaller acceptance angle of the analyzer (an acceptance angle of ±2° was used in Ref. 20 and an acceptance angle of ±8° was used in Ref. 25).

Since the intensity ratio of surface components gives information about the number of corresponding Si atoms in the unit cell and thus more accurate information about the atomic structure, we pay attention to the intensity ratio of the S1 and S2 components. In the present study, the intensity ratio of S1 and S2 was approximately 7:1 using a photon energy of 135 eV and approximately 2:1 using $h\nu=125$ and 145 eV. By comparing the intensity ratio obtained with $h\nu=135$ eV and other photon energies, one notices that the intensity of S1 is obviously enlarged at $h\nu=135$ eV due to a diffraction effect. In contrast to the photon energy-dependent diffraction effect, the intensity ratio of S1 and S2 was insensitive to θ_e . These results indicate that the original intensity ratio of S1 and S2 is 2:1, i.e., the same ratio as that reported for the Ca/Si(111)-(3×2) surface. Moreover, since the 7:1 intensity ratio of the S1 and S2 components was not observed on the 1/3 ML monovalent atom induced HCC structure and it was just observed at a photon energy of 135 eV,^{14,20,25,35} we conclude that this ratio results from a diffraction effect that is peculiar to the 1/6 ML divalent atom induced HCC structure.

The difference between this intensity ratio and that reported for the Ba induced (3×2) surface²⁵ might result from the different quality of the sample. That is, a surface component, which is only observed in the intermediate phase on the Eu/Si(111) and Ca/Si(111) surfaces, is clearly observed in the spectra of the Ba/Si(111)-(3×2) surface. Since the intensity of S2 becomes larger in the Eu and Ca induced intermediate phases as shown in Fig. 5 and in Ref. 20, we suspect that the intensity of S2 is overestimated due to the contribution from the intermediate Ba/Si(111)-(5×1) phase in Ref. 25. The intensity ratio of 2:1 indicates that the number ratio of Si atoms that produce S1 and S2 is 2:1 in the (3×2) phase. This ratio fits the number ratio of the *b* and *a* Si atoms [Fig. 1(a)] per unit cell, and we, therefore, conclude that the origin of S1 is the *b* Si atoms and the origin of S2 is the *a* Si atoms, likewise the attributions reported on the Ca/Si(111)-(3×2) surface²⁰ and the recent study on the Eu/Si(111)-(3×2) surface.¹⁴

The S3 component was reported to originate from the Si atoms, which form the honeycomb, but are not bonded to the adsorbate for the 1/3 ML monovalent atoms induced Si(111)-(3×1) surfaces^{6,28,35} and the 1/6 ML AEM's induced Si(111)-(3×2) surfaces^{20,25} [the *c* and *d* Si atoms shown in Fig. 1(a)]. On the other hand, S3 is stated to originate from the second and third layers Si atoms situated below the adsorbate in a theoretical calculation done for the 1/3 ML Ca adsorbed Si(111)-(3×1) surface,³⁰ i.e., the *e* and *f* Si atoms. The intensity ratio of S1, S2, and S3 was approximately 2:1:4 in the Si 2*p* core-level spectrum obtained using $h\nu=145$ eV and approximately 2:1:3 using $h\nu=125$ eV. These ratios indicate that the number of Si atoms, which produce S3, is four per unit cell at most. In the theoretical calculation performed in Ref. 30, a metallic surface has been assumed in spite of the semiconducting electronic character of this surface. This assumption used in Ref. 30 leads to an overestimation of the screening effect and, thus, suggests that the *e* and *f* Si atoms might be unsuitable for the origin of S3. However, since we cannot exclude the possibility of other origins completely, we state that S3 *mainly originates* from the *c* and *d* Si atoms in the (3×2) phase.

B. Eu/Si(111)-(2×1)

The highest coverage phases induced by the adsorption of divalent atoms on a Si(111) surface show different reconstructions. Ca,^{20,30–32,36,37} Sr,³⁸ Yb,^{7,8} and Eu^{10–13} form a (2×1) reconstruction, while the adsorption of Ba leads to a (2×8) reconstruction.^{25,39} The origin of this difference was proposed to be either the large ionic radius of Ba that induces a strain relaxation within the (2×1) unit cell,²⁵ or the disorder of the ×8 periodicity caused by defects in the Ca, Sr, Yb, and Eu adsorbed surface.³⁹ The second proposition is based on the fact that the ×8 spots are weaker than the ×2 spots so that the ×8 spots may disappear in the diffuse background and, thus, suggests that all divalent atoms induced highest coverage phase have the (2×8) reconstruction. However, the highest coverage Eu induced phase shows a clear (2×1) LEED pattern with a quite low background in Fig. 2(a). Therefore, we conclude that the (2×8) reconstruction is only formed by the adsorption of Ba, and the other divalent atoms, whose ionic radii are smaller than that of Ba, form a (2×1) reconstruction. (The ionic radius of Eu with a valence state of 2+ is almost the same as that of Sr, but smaller than that of Ba, and the ionic radii of Ca and Yb are smaller than those of Eu²⁺ and Sr.)

On the Ca/Si(111)-(2×1) surface,²⁰ three surface components were observed in the Si 2*p* core-level spectra. The binding energies of two of them are smaller than that of the bulk component and the binding energy of one surface component is larger. As shown in Fig. 5, the same number of surface components is observed in each side of the bulk component on the Eu/Si(111)-(2×1) surface. This result indicates that the atomic structures of the Eu and Ca induced Si(111)-(2×1) surfaces are similar and, thus, supports that the atomic structure of the (2×1) phase is the Seiwatz structure with an Eu coverage of 0.5 ML.

Of the three surface components, the intensity ratio of S1 and S2 was approximately 2:1 using $h\nu=135$ eV and approximately 1:1 using other photon energies. Since the intensity ratio obtained with other photon energies was identical and the ratios were insensitive to θ_e , the original intensity ratio of S1 and S2 should be 1:1 on the Eu/Si(111)-(2×1) surface. The intensity ratio of the two corresponding surface components observed on the Ca/Si(111)-(2×1) surface is 1:1 as well, and the atomic structures of the Eu and the Ca induced (2×1) surfaces are similar. Based on these similarities, we attribute S1 and S2 to originate from the *h* and *g* Si atoms shown in Fig. 1(b), respectively, likewise the attributions done on the Ca/Si(111)-(2×1) surface. Here, we notice that the relative binding energy of S1 is similar to the binding energy of its corresponding component on the Ca/Si(111)-(2×1) surface, whereas the relative binding energy of S2 is different from that of its corresponding component. Since a difference in magnitude of buckling for Si atoms forming Seiwatz chains leads to a different “adsorbate-Si” distance and, thus, a different amount of transferred charges, we propose that the difference in the relative binding energy of S2 results from the different magnitude of buckling.

Regarding S3, its intensity showed a strong photon energy dependence due to a diffraction effect. The intensity ratio of S1, S2, and S3 was approximately 1:1:2.5 using $h\nu=145$ eV and approximately 1:1:1 using $h\nu=125$ eV. This means that we cannot discuss the number of Si atoms that produce the S3 component based on its intensity. In the theoretical calculation performed for the 0.5 ML Ca induced Si(111)-(2×1) surface,³⁰ the corresponding component was attributed to originate from the Si atoms situated just below the adsorbate. Therefore, although we do not have any strong evidence, we attribute S3 of the Eu/Si(111)-(2×1) surface to the *i* atoms shown in Fig. 1(b).

C. Eu/Si(111)-(5×4)

Although different structural models have been proposed for the so-called (5×1) phase that is formed by the adsorption of divalent atoms, the basic structure of these models is the same, i.e., the atomic structure of the Si atoms follows the HCC and Seiwatz models. As mentioned above, the origin of each Si 2*p* surface component is the same or quite similar in the Eu induced (2×1), (5×4), and (3×2) phases. This result suggests that the basic structure of the Eu induced (5×4) phase is also formed by a combination of the HCC and Seiwatz models. The difference in the proposed (5×1) models mainly results from the different adsorbate coverage and the different adsorption site. (The adsorbate coverages were reported to be 0.3 ML for the Ca induced reconstruction,²⁰ 0.2 ML for the Ba induced one,²⁵ and 0.4 ML for the Eu induced phase.^{12–14})

Since the adsorbate coverage is essential to determine the atomic structure of the Eu/Si(111)-(5×4) surface, we first reinvestigate the Eu coverage of the (5×4) phase based on the Eu core-level spectra. The intensity ratio of the Eu 4*f* core-level is 1:0.57:0.31 for the (2×1), (5×4), and (3×2) phases (Fig. 3). A quite similar intensity ratio [1:0.62:0.33

for the (2×1) , (5×4) , and (3×2) phases] was also obtained in the Eu $5p$ core level spectra. Taking into account that the coverages of the (2×1) and (3×2) phases are 0.5 ML and $1/6$ ML, respectively, the intensity ratios of the Eu core levels indicate that the Eu coverage of the (5×4) phase is $0.3(\pm 0.015)$ ML. By considering the so-called (5×1) phase into two parts, i.e., the HCC part and the Seiwatz part, a 0.3 ML coverage corresponds to the donation of one electron per honeycomb in the HCC part and the donation of two electrons in the unoccupied surface band of a π -bonded chain in the Seiwatz part. These numbers agree well with the numbers of electrons that stabilize each part, and thus support that the adsorbate coverage of the (5×4) phase is 0.3 ML (e.g., a higher coverage would lead to the donation of more than one electron per honeycomb and thus makes the HCC structure unstable). We, therefore, conclude that the Eu coverage of the (5×4) phase is 0.3 ML, and the coverage reported in the previous studies^{10,13,14} was overestimated.⁴⁰ Further, the adsorbate coverage of 0.3 ML indicates that the structural model proposed for the so-called Eu/Si(111)- (5×1) surface in the literature [Fig. 1(c)] is no longer applicable.

The energy shift of S4 is larger than that of S1 and S2. On the Ba/Si(111) surfaces,²⁵ the corresponding component was attributed to originate from either a small portion of silicide or a defect structure based on its presence in all phases. However, the S4 component is only observed in the intermediate (5×4) phase in the present study (Figs. 4 and 5) as well as the result on the Ca induced phases.²⁰ This observation indicates that S4 is a component peculiar to the intermediate phase, and the proposition reported in Ref. 25 is no longer valid in the present case. A possible assignment of the origin of S4 is the Si atoms with a larger amount of charge transferred from Eu. Such large charge can be transferred in the case of a larger number of surrounding Eu atoms per Si atom and/or a larger overlap between the Eu s orbital and the Si dangling bond that is formed by a shorter Eu-Si distance. All Eu atoms are adsorbed on the T_4 site in the (3×2) and (2×1) phases [Figs. 1(a) and 1(b)], and thus more than one Eu adsorption site is needed to have Si atoms with a larger amount of transferred charge in the (5×4) phase. The presence of more than one adsorption site is consistent with the result shown in Fig. 3, i.e., the $\text{Eu}^{2+}4f$ peak of the (5×4) phase is well reproduced by two calculated $\text{Eu}^{2+}4f$ peaks whose intensity ratio is 2:1. Taking into account that the origins of S1 and S2 observed in the (5×4) phase should be the same or quite similar to those of the S1 and S2 observed in the two end phases, the small intensity of S4 and the 2:1 intensity ratio of the $\text{Eu}^{2+}4f$ peaks suggest that among the six Eu atoms in the (5×4) unit cell, four of them are adsorbed on the T_4 site and two on another site.

Based on the (5×4) periodicity and the presence of two adsorption sites, we propose two structural models for the (5×4) phase in Fig. 6. In the left part of Fig. 6, 0.2 ML of Eu is adsorbed on the T_4 site and 0.1 ML on the H_3 site (H_3 model), and in the right part, 0.2 ML of Eu is adsorbed on the T_4 site and 0.1 ML on the B_2 site (B_2 model). By considering the size of the filled circles, which almost represents the ionic radius of Eu^{2+} , one notices that the distance between an Eu atom adsorbed on the H_3 site and the Eu atom

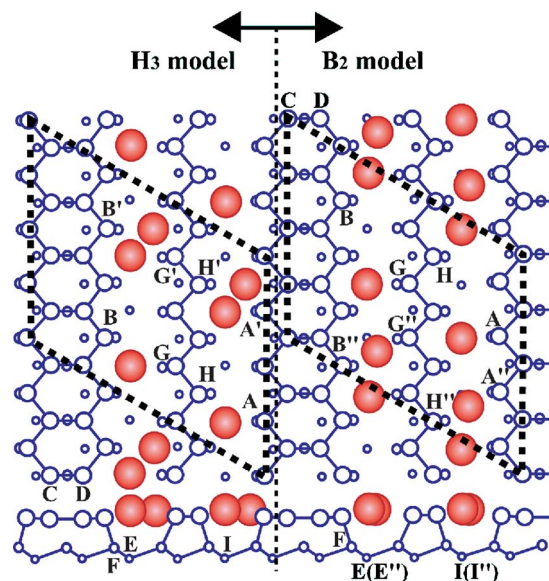


FIG. 6. (Color online) Structural models for the Eu/Si(111)- (5×4) surface with a coverage of 0.3 ML. The atomic structure of Si atoms is a combination of the HCC structure and the Seiwatz structure. Filled circles are Eu atoms, and open circles are Si atoms. In the left part, 0.2 ML of Eu is adsorbed on the T_4 site and 0.1 ML on the H_3 site (H_3 model). In the right part, 0.2 ML Eu is adsorbed on the T_4 site and 0.1 ML on the B_2 site (B_2 model). The bold dashed lines indicate the unit cell in each model.

adsorbed on the nearest T_4 site is quite close. Since the adsorbed Eu atoms are positively charged, the short Eu-Eu distance suggests that although the adsorption on the H_3 site was reported to be more stable than the adsorption on the B_2 site in the theoretical calculation performed for the Ba/Si(111)- (3×2) surface,¹⁸ the H_3 site might not be the more stable adsorption site in the present case. That is, we cannot exclude the possibility of the B_2 model using this theoretical calculation.

In the H_3 model, the A' , B' , G' , and H' Si atoms are surrounded by two Eu atoms, while the A - I Si atoms are in the same environments as the surface Si atoms in the (3×2) and (2×1) phases. This means that the A' , B' , G' , and H' Si atoms are candidates for the origin of S4 in the H_3 model. In the B_2 model, the B'' and H'' Si atoms are surrounded by two Eu atoms, the A'' , E'' , G'' , and I'' Si atoms are in a slightly different environments as those in the (3×2) and (2×1) phases, and the A - I Si atoms are in the same environments as those in the two end phases. By considering that the Eu-Si(A'') and Eu-Si(G'') distances are almost the same as those of Eu-Si(A) and Eu-Si(G), the candidates for the origin of S4 are the B'' and H'' Si atoms in the B_2 model. The intensity ratio of S1, S2, and S4 varies from 2:3:1 to 2:4:1 depending on the experimental condition ($h\nu$ and E_B). Taking the number of Si atoms that face the adsorbate into account, these ratios indicate that surface Si atoms that produce the S4 component should be less than three per unit cell. This means that the B_2 model is more appropriate, and we, therefore, attribute the origin of S4 to the B'' and H'' Si atoms, which are surrounded by two Eu atoms.

The A and B Si atoms have the same coordination as the a and b Si atoms of the (3×2) phase, and the G Si atoms

have the same coordination as the g atoms of the (2×1) phase. The equivalencies in coordination indicate that the B atoms produce S1, and the A and G atoms produce S2. On the other hand, the Eu-Si distances of the A'' and G'' Si atoms are slightly shorter than those of the A and G atoms, and the coordination of the H atoms is slightly different from that of the h atoms of the (2×1) phase, i.e., only one Eu atom is adsorbed near the H atoms whereas two Eu atoms are situated near the h atoms. A shorter distance suggests a larger amount of charge transfer into these Si atoms, and a lower number of surrounding Eu atoms per Si atom suggests a lower amount of charge transfer. Thus, by assuming that the amount of charge transfer into the A'' and G'' Si atoms is almost the same as the amount transferred into the B atoms, the A'' and G'' atoms might also contribute to S1. Further, by assuming that the amount of charge transfer into the H atoms is almost the same as the amount transferred into the A and G atoms, the H atoms might contribute to S2. The ratio of $(B + A'' + G''):(A + G + H):(B'' + H'')$ is 5:7:2, and this ratio is in good agreement with the intensity ratio of S1, S2, and S4. Therefore, we attribute S1 and S2 of the (5×4) phase to the combinations of $(B + A'' + G'')$ and $(A + G + H)$, respectively.

The S5 component, which is only observed in the intermediate phases in similarity with S4, shows the highest binding energy. In the (2×1) phase, the second layer Si atoms situated just below the Eu atoms have contributions to the highest binding energy components. The distance between Eu and the Si atoms below the Eu is slightly longer in the case of B_2 site adsorption compared with the case of T_4 site adsorption. This difference can change the charge states of the second layer Si atoms. Thus, although there is no strong evidence, we propose the origin of S5 to be the E'' and I'' atoms that are situated below the Eu atoms adsorbed on the B_2 site.

V. CONCLUSIONS

In conclusion, we have studied the atomic structures of the so-called Eu/Si(111)- $(n \times 1)$ surfaces by LEED and

high-resolution core-level photoelectron spectroscopy. Depending on the Eu coverage, the (3×2) , (5×4) , (9×1) , (11×1) , and (2×1) phases were observed in LEED. The Eu 4*f* core-level spectra show that the valence state of the adsorbate is 2+ in the (3×2) , (5×4) , and (2×1) phases. In the Si 2*p* core-level spectra, three surface components were observed in both the (3×2) and (2×1) phases. By considering the energy shift and intensity of each Si 2*p* surface component and the intensity of the Eu 4*f* core level, we conclude that the structure of the (3×2) phase is given by the HCC model with an Eu coverage of 1/6 ML, and the (2×1) phase is formed by π -bonded Seiwatz Si chains with a coverage of 0.5 ML. Regarding the (5×4) phase, the observation of the $\times 4$ periodicity in LEED, the 0.3 ML Eu coverage that is obtained from the Eu core-level spectra, and the presences of the S4 and S5 in the Si 2*p* core-level spectra indicate that the atomic structure of this phase is basically formed by a combination of the HCC and Seiwatz models, while not all Eu atoms are adsorbed on the T_4 site. Taking the energy shifts and intensities of S4 into account, we have proposed a structural model of the (5×4) phase, in which two Eu atoms are adsorbed on the B_2 site and four on the T_4 site per unit cell.

ACKNOWLEDGMENTS

Experimental support from Dr. T. Balasubramanian, Dr. J. He, and the MAX-lab staff, suggestions on the sample preparation from Dr. K. Shimada, and fruitful discussion with Dr. K. Mimura are gratefully acknowledged. This work was financially supported by the Swedish Research Council and the Ministry of Education, Culture, Sports, Science, and Technology of the Japanese Government. K.S. was partially supported by the MEXT 21st Century COE Program "Exploring New Science by Bridging Particle-Matter Hierarchy."

*Corresponding author. Present address: Graduate School of Science and Technology, Chiba University, Chiba 263-8522, Japan. Electronic address: kazuyuki_sakamoto@faculty.chiba-u.jp.

¹P. Segovia, D. Purdie, M. Hengsberger, and Y. Baer, *Nature (London)* **402**, 504 (1999).

²H. W. Yeom, S. Takeda, E. Rotenberg, I. Matsuda, K. Horikoshi, J. Schaefer, C. M. Lee, S. D. Kevan, T. Ohta, T. Nagao, and S. Hasegawa, *Phys. Rev. Lett.* **82**, 4898 (1999).

³O. Gallus, Th. Pillo, M. Hengsberger, P. Segovia, and Y. Baer, *Eur. Phys. J. B* **20**, 313 (2001).

⁴R. Losio, K. N. Altmann, A. Kirakosian, J. L. Lin, D. Y. Petrovykh, and F. J. Himpsel, *Phys. Rev. Lett.* **86**, 4632 (2001).

⁵I. K. Robinson, P. A. Bennett, and F. J. Himpsel, *Phys. Rev. Lett.* **88**, 096104 (2002).

⁶K. Sakamoto, H. Ashima, H. M. Zhang, and R. I. G. Uhrberg, *Phys. Rev. B* **65**, 045305 (2002).

⁷C. Wigren, J. N. Andersen, R. Nyholm, M. Göthelid, M. Ham-

mar, C. Törnevik, and U. O. Karlsson, *Phys. Rev. B* **48**, 11014 (1993).

⁸C. Wigren, J. N. Andersen, R. Nyholm, U. O. Karlsson, J. Nogami, A. A. Baski, and C. F. Quate, *Phys. Rev. B* **47**, 9663 (1993).

⁹M. Kuzmin, P. Laukkanen, R. E. Perälä, and I. J. Väyrynen, *Surf. Sci.* **515**, 471 (2002).

¹⁰T. V. Krachino, M. V. Kuz'min, M. V. Loginov, and M. A. Mittsev, *Appl. Surf. Sci.* **182**, 115 (2001).

¹¹M. Kuzmin, R-L. Vaara, P. Laukkanen, R. E. Perälä, and I. J. Väyrynen, *Surf. Sci.* **538**, 124 (2003).

¹²R-L. Vaara, M. Kuzmin, P. Laukkanen, R. E. Perälä, and I. J. Väyrynen, *Appl. Surf. Sci.* **220**, 327 (2003).

¹³M. Kuzmin, R-L. Vaara, P. Laukkanen, R. E. Perälä, and I. J. Väyrynen, *Surf. Sci.* **549**, 183 (2004).

¹⁴M. Kuzmin, P. Laukkanen, R. E. Perälä, R-L. Vaara, and I. J. Väyrynen, *Phys. Rev. B* **71**, 155334 (2005).

- ¹⁵K. Sakamoto, A. Pick, and R. I. G. Uhrberg, *Phys. Rev. B* **72**, 045310 (2005).
- ¹⁶F. Palmino, E. Ehret, L. Mansour, J-C. Labrune, G. Lee, H. Kim, and J-M. Themlin, *Phys. Rev. B* **67**, 195413 (2003).
- ¹⁷T. Okuda, H. Ashima, H. Takeda, K. S. An, A. Harasawa, and T. Kinoshita, *Phys. Rev. B* **64**, 165312 (2001).
- ¹⁸G. Lee, S. Hong, H. Kim, D. Shin, J-Y. Koo, H-I. Lee, and Dae Won Moon, *Phys. Rev. Lett.* **87**, 056104 (2001).
- ¹⁹J. Schäfer, S. C. Erwin, M. Hansmann, Z. Song, E. Rotenberg, S. D. Kevan, C. S. Hellberg, and K. Horn, *Phys. Rev. B* **67**, 085411 (2002).
- ²⁰K. Sakamoto, W. Takeyama, H. M. Zhang, and R. I. G. Uhrberg, *Phys. Rev. B* **66**, 165319 (2002).
- ²¹D. Y. Petrovykh, K. N. Altmann, J-L. Lin, F. J. Himpsel, and F. M. Leibsle, *Surf. Sci.* **512**, 269 (2002).
- ²²O. Gallus, Th. Pillo, P. Starowicz, and Y. Baer, *Europhys. Lett.* **60**, 903 (2002).
- ²³Y. K. Kim, J. W. Kim, H. S. Lee, Y. J. Kim, and H. W. Yeom, *Phys. Rev. B* **68**, 245312 (2003).
- ²⁴K. Sakamoto, H. M. Zhang, and R. I. G. Uhrberg, *Phys. Rev. B* **69**, 125321 (2004).
- ²⁵T. Okuda, K-S. An, A. Harasawa, and T. Kinoshita, *Phys. Rev. B* **71**, 085317 (2005).
- ²⁶S. C. Erwin and H. H. Weitering, *Phys. Rev. Lett.* **81**, 2296 (1998).
- ²⁷L. Lottermoser, E. Landemark, D-M. Smilgies, M. Nielsen, R. Feidenhans'l, G. Falkenberg, R. L. Johnson, M. Gierer, A. P. Seitonen, H. Kleine, H. Bludau, H. Over, S. K. Kim, and F. Jona, *Phys. Rev. Lett.* **80**, 3980 (1998).
- ²⁸M-H. Kang, J-H. Kang, and S. Jeong, *Phys. Rev. B* **58**, R13359 (1998).
- ²⁹R. Seiwatz, *Surf. Sci.* **2**, 473 (1964).
- ³⁰A. A. Baski, S. C. Erwin, M. S. Turner, K. M. Jones, J. W. Dickinson, and J. A. Carlisle, *Surf. Sci.* **476**, 22 (2001).
- ³¹T. Sekiguchi, F. Shimokoshi, T. Nagao, and S. Hasegawa, *Surf. Sci.* **493**, 148 (2001).
- ³²K. Sakamoto, H. M. Zhang, and R. I. G. Uhrberg, *Phys. Rev. B* **68**, 245316 (2003).
- ³³F. Gerken, *J. Phys. F: Met. Phys.* **13**, 703 (1983).
- ³⁴See, for example, N. Mårtensson, B. Reihl, W-D. Schneider, V. Murgai, L. C. Gupta, and R. D. Parks, *Phys. Rev. B* **25**, 1446 (1982).
- ³⁵K. Sakamoto, H. M. Zhang, and R. I. G. Uhrberg, *Surf. Rev. Lett.* **9**, 1235 (2002).
- ³⁶M. A. Olmstead, R. I. G. Uhrberg, R. D. Bringans, and R. Z. Bachrach, *Phys. Rev. B* **35**, 7526 (1987).
- ³⁷G. C. L. Wong, C. A. Lucas, D. Loretto, A. P. Payne, and P. H. Fuoss, *Phys. Rev. Lett.* **73**, 991 (1994).
- ³⁸M. A. Olmstead and R. D. Bringans, *Phys. Rev. B* **41**, 8420 (1990).
- ³⁹H. H. Weitering, *Surf. Sci.* **355**, L271 (1996).
- ⁴⁰The coverages of the (3×2) and (5×1) phases were obtained to be 0.2 and 0.4 ML experimentally in the previous studies. This means that not only the coverage of the intermediate phase, but also the coverage of the (3×2) phase was overestimated. By considering the 1/6 ML coverage of the (3×2) phase, the 0.2:0.4 ratio suggests that the Eu coverage of the (5×4) phase is 0.33 ML, a coverage close to that obtained in the present study.